arXiv:1401.5901v1 [cond-mat.stat-mech] 23 Jan 2014

First passage statistics for aging diffusion in annealed and quenched disorder

Henning Krüsemann,[1] Aljaž Godec,[1,2] and Ralf Metzler[1,3,*]

[1] *Institute of Physics & Astronomy, University of Potsdam, 14776 Potsdam-Golm, Germany*
[2] *National Institute of Chemistry, 1000 Ljubljana, Slovenia*
[3] *Department of Physics, Tampere University of Technology, FI-33101 Tampere, Finland*

(Dated: January 24, 2014)

Aging, the dependence of the dynamics of a physical process on the time t_a since its original preparation, is observed in systems ranging from the motion of charge carriers in amorphous semiconductors over the blinking dynamics of quantum dots to the tracer dispersion in living biological cells. Here we study the effects of aging on one of the most fundamental properties of a stochastic process, the first passage dynamics. We find that for an aging continuous time random walk process the scaling exponent of the density of first passage times changes twice as the aging progresses and reveals an intermediate scaling regime. The first passage dynamics depends on t_a differently for intermediate and strong aging. Similar crossovers are obtained for the first passage dynamics for a confined and driven particle. Comparison to the motion of an aged particle in the quenched trap model with a bias shows excellent agreement with our analytical findings. Our results demonstrate how first passage measurements can be used to unravel the age t_a of a physical system.

PACS numbers: 72.20.Jv,72.70.+m,89.75.Da,05.40.-a

In their groundbreaking 1975 paper Scher and Montroll introduced the scale-free distribution $\psi(\tau) \simeq \tau^{-1-\alpha}$ with $0 < \alpha < 1$ of trapping (waiting) times τ for moving charge carriers in amorphous semiconductors to explain the measured power-law form of the electrical current [1, 2]. This then radical assumption has since then been verified in numerous systems [3] including the tracer dispersion in groundwater aquifers [4], the motion of endogenous protein channels and granules in biological cells [5, 6] and of submicron tracers in structured environments [7], or the blinking dynamics of quantum dots [8].

The lack of a time scale $\langle\tau\rangle$ in these systems effects the disparity between ensemble and time averages of physical observables (weak ergodicity breaking) [9, 10] and an explicit dependence of observables on the time span between the initial preparation of the system and start of the measurement at t_a, the so-called aging [11–13]. Aging phenomena can be rationalized by particle dynamics in quenched energy landscapes [14] or logistic maps [15], and were experimentally observed in biological systems [5] as well as amorphous semiconductors [16].

Here we present analytical and numerical evidence for the distinct effects of aging on the first passage properties of aging systems, i.e., the statistics of the times when the process first crosses a pre-set value. In the above examples this is the arrival of charge carriers at the counterelectrode, giving rise to the decay of the electrical current, the breakthrough of chemical tracers at some probe location in an aquifer, the arrival of a protein channel at a specific receptor in a cell membrane, or for a quantum dot to reach its nth on-state. Our results for the first passage time density (FPTD) $\wp(t)$ in systems with a diverging time scale $\langle\tau\rangle$ exhibit a clear dependence on the aging time t_a in the cases of intermediate and strong aging while $\wp(t)$ is independent of t_a for short aging times. More importantly, progressing aging changes the scaling exponent of $\wp(t)$ and reveals an interesting intermediate scaling regime. For biased diffusion we show that our results agree well with simulations in a quenched energy landscape. Finally we address the question how first passage measurements can be used to unravel information on the age t_a of the observed system.

In the absence of aging ($t_a = 0$), i.e., when the measurement commences simultaneously with the initiation of the system at $t = 0$, the Scher-Montroll continuous time random walk (CTRW) process with trapping time density $\psi(\tau) \simeq \tau^{-1-\alpha}$ and $0 < \alpha < 1$ causes free anomalous diffusion of the subdiffusive form $\langle x^2(t)\rangle \simeq K_\alpha t^\alpha$, with the anomalous diffusion coefficient K_α [1, 3]. On the semi-axis with δ-initial condition at $x = 0$ the FPTD to the point x_0 associated with this CTRW process reads

$$\wp(t) = \left(\frac{K_\alpha}{x_0^2}\right)^{1/\alpha} l_{\alpha/2}\left(\left[\frac{K_\alpha}{x_0^2}\right]^{1/\alpha} t\right) \simeq \frac{x_0/K_\alpha^{1/2}}{t^{1+\alpha/2}} \quad (1)$$

in terms of the one-sided Lévy stable law $l_{\alpha/2}(t)$ [17]. Its asymptotic expansion shows the power-law decay $t^{-1-\alpha/2}$ characteristic for unbiased subdiffusion [3]. Eq. (1) follows from the Laplace image [18] $\wp(u) = \exp(-x_0 u^{\alpha/2} K_\alpha^{1/2})$ derived in Ref. [19]. In the Brownian limit $\alpha = 1$, the FPTD reduces to the familiar Lévy-Smirnov law with asymptote $\wp(t) \simeq x_0/[K_1 t^{3/2}]$ exhibiting the famed Sparre-Andersen 3/2 universality [20].

To extend this result for an aged system ($t_a > 0$) we use the propagator described by the aging CTRW [12, 21]

$$P_a(k, s, u) = P_0(s, u) + h(s, u)[u + K_\alpha u^{1-\alpha} k^2]^{-1} \quad (2)$$

in Fourier-double Laplace representation $P_a(x, t_a, t) \to P(k, s, u)$ [22]. The major component in the mathematical description of aging processes is the density $h(t_a, t)$

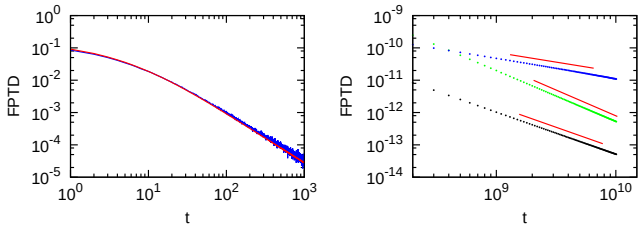

FIG. 1: Semi-infinite domain. Left: Simulation (blue) and analytical result (red) for $\alpha = 0.75$, $t_a = 100$, $x_0 = 1$, and $K_\alpha = 0.5$. Right: Different scaling regimes in the long time limit for $t_a = 0.1$ (black, bottom), $t_a = 10^7$ (green, middle), and $t_a = 10^{11}$ (blue, top), with $\alpha = 0.6$, $x_0 = 1$, $K_\alpha = 0.2$.

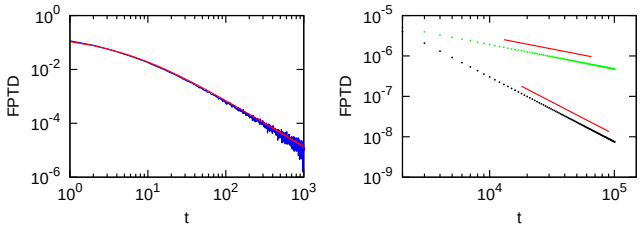

FIG. 2: Finite domain. Left: Simulation (blue) and analytical result (red) for $\alpha = 0.75$, $t_a = 100$, $x_0 = 1$, and $K_\alpha = 0.5$. Right: Different scaling regimes in the long time limit for $t_a = 0.1$ (black, bottom) and $t_a = 10^7$ (green, top), with $\alpha = 0.6$, $x_0 = 1$, $K_\alpha = 0.2$.

for the so-called forward waiting time t for the occurrence of the first step in the random walk process, after the system aged for t_a. Due to the lack of a characteristic scale of ψ increasingly longer trapping times occur while the system evolves. Typically, after the aging period the system is arrested in such a long trapping state, thus changing the statistics of the first step to occur, as given by the distribution h. Its double Laplace transform is $h(s,u) = [\psi(s) - \psi(u)]/([u-s][1-\psi(s)]$ [12, 21]. In Eq. (2) $P_0(s,u) = [1 - sh(s,u)]/(su)$ is the Laplace transform of the probability $P_0(t_a,t)$ that no step occurs up to time t. The splitting into a discrete part for completely immobile particles and a continuous portion weighted by the density h is typical for aging CTRW processes [21].

Using the standard method of images [20] and the subordination trick [3, 23] we find the general closed form

$$\wp_a(t_a,t) = \left(\frac{K_\alpha}{x_0^2}\right)^{1/\alpha} h(t_a,t) \otimes l_{\alpha/2}\left(\left(\frac{K_\alpha}{x_0^2}\right)^{1/\alpha} t\right) \quad (3)$$

for the FPTD, where $\otimes$ denotes a Laplace convolution. This form is very useful for numerical evaluation. The exact expression for $\wp_a(t_a,t)$ involves an infinite power series [24]. In the long time limit ($t \to \infty$) we find the three scaling regimes

$$\wp_a(t_a,t) \simeq \begin{cases} t_a^{\alpha-1} t^{-\alpha}, & t_a \gg t \\ t_a^{\alpha} t^{-1-\alpha}, & t_a \ll t \ll t_a^2 \\ x_0 K_\alpha^{-1/2} t^{-1-\alpha/2}, & t_a^2 \ll t \end{cases} \quad (4)$$

depending on the severity of the aging. Thus, when aging is weak, the asymptotic behavior of the non-aged process from Eq. (1) is preserved. Remarkably, once the aging becomes more pronounced, the competition between the magnitudes of the measurement time t and the aging time t_a effects a change of the scaling exponent of t from $1+\alpha/2$ to $1+\alpha$ at intermediate values of t_a, and a further change to α under strong aging conditions. The crossover between these scaling regimes is a key signature of scale-free CTRW processes. Fig. 1 on the left demonstrates excellent agreement of our analytical result (3) with simulations of the CTRW process with trapping time density $\psi(\tau)$. On the right of Fig. 1 we confirm the existence of the three different scaling regimes of $\wp(t)$ predicted by Eq. (4), again observing excellent agreement. Note, however, that in order to see all three regimes, the variation of t_a needs to be quite large. Thus, depending on the physical system and the experimental technique not all three regimes may be detectable. As the first crossover in Eq. (4) increases the magnitude of the scaling exponent while the second crossover decreases it again, the FPTD behavior nevertheless provides a new method to deduce the age t_a of an aging system. The discovery of three distinct scaling regimes and the dependence of the FPTD on the aging time t_a are our first main results.

Finite domain. For the first passage to the boundaries of a finite domain the asymptotic scaling of the non-aged FPTD is $\wp(t) \simeq x_0^2 K_\alpha^{-1} t^{-1-\alpha}$ [19], i.e., the decay is steeper than in the semi-infinite case. Due to the divergence of the trapping time scale $\langle\tau\rangle$, however, the mean first passage time still diverges, in contrast to the Brownian case ($\alpha = 1$), for which $\wp(t)$ has an exponential cutoff [20]. For the aged system, we again derive $\wp_a(t_a,t)$ via the images method. From a convolution similar to Eq. (3) we find an exact solution in terms of a power series with Lerch functions [24]. The long-time scaling

$$\wp_a(t_a,t) \simeq \begin{cases} t_a^{\alpha-1} t^{-\alpha}, & t_a \gg t \\ (x_0^2/[2K_\alpha] + t_a^\alpha/\Gamma(1+\alpha)) t^{-1-\alpha}, & t_a \ll t \end{cases} \quad (5)$$

emerges, where this time we only observe two scaling regimes in the measurement time t: at weak aging, the scaling exponent is $1+\alpha$, which changes to α at strong aging. Concurrently the aging time does not appear explicitly as long as $t_a \ll (x_0^2\Gamma(1+\alpha)/[2K_\alpha])^{1/\alpha}$. At intermediate aging, the prefactor $t_a^{-\alpha}$ enters, while for strong aging it changes to $t_a^{-1-\alpha}$. Fig. 2 shows excellent agreement with these results. The behavior of the aged FPTD on a finite domain is our second important result.

Biased diffusion. In many physical systems the motion of the particle is biased by an external force, for instance, the electrical field acting on the charge carriers in the amorphous semiconductor of Ref. [1] or a subsurface water stream dragging along the dissolved tracer chemicals in groundwater aquifers [4]. To explore the effects of an

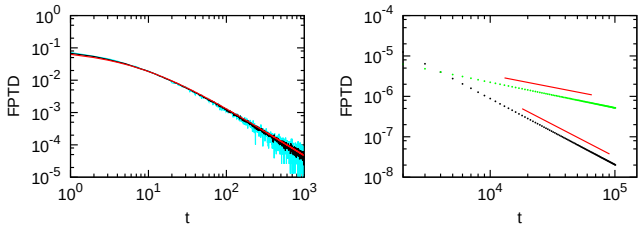

FIG. 3: Semi-infinite domain, biased case. Left: Simulations of quenched trap model (cyan) and CTRW (black), and analytical result (red), for $\alpha = 0.5$, $t_a = 100$, $F = 1$, $T = 0.5$, $x_0 = 0.2$, $\tau_0 = 10^{-4}$. Right: Different scaling regimes for $t_1 = 0.1$ (black, bottom) and $t_a = 10^7$ (green, top), for $\alpha = 0.6$, $x_0 = 1$ and $K_\alpha = 0.2$.

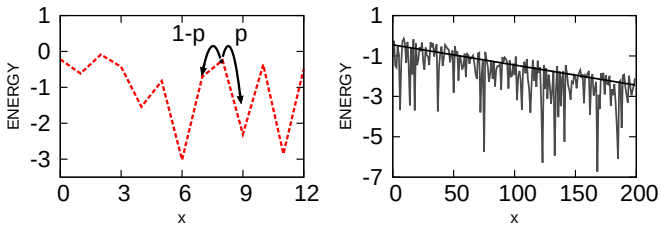

FIG. 4: Left: Schematic motion in quenched trap model with energy-dependent transition probabilities $1-p$ and p for moving to the left and right. Right: Realization of the tilted quenched trapped model with $T_g = 1$, $F = 1$, and $a = 10^{-3}$. The lattice constant in this Figure is 2, while we chose 0.01 in the simulations for Fig. 3.

external bias on the FPTD we now add the force F to the dynamics. In the classical Brownian case, a bias towards the absorbing boundary leads to an exponential decay of the associated FPTD, with the mean first passage time $x_0 m\eta/F$, where η is the friction coefficient. In the non-aged case with a scale-free distribution $\psi(\tau)$ of trapping times, the FPTD has the power-law form $\wp(t) \simeq x_0 t^{-1-\alpha}$ and the mean first passage time diverges. When the system is aged, the method of images with an appropriate correction factor still applies [20] and we find the FPTD

$$\wp_a(t_a, t) = h(t_a, t) \otimes \{\otimes_{k=1}^{\infty} g_k(t)\} \tag{6}$$

as a multiple convolution $\otimes_{k=1}^{n} g_k(t) = g_1 \otimes g_2 \otimes \cdots \otimes g_n(t)$ of the function $g_k(t) = \mathcal{D}(\alpha, k) l_{k\alpha}\big(\mathcal{D}(\alpha, k)t\big)$ with [25]

$$\mathcal{D}(\alpha, k) = \left[\left(\frac{2T}{F}\right)^{2k-1} \left(\frac{2}{K_\alpha}\right)^{k} \frac{\Gamma(3/2)}{\Gamma(3/2-k)k!} \right]^{-1/k\alpha} . \tag{7}$$

Here, the temperature T enters due to the competition between the force F and the thermal energy $k_B T$ included through the generalized Einstein-Stokes relation $K_\alpha = k_B T/(m\eta_\alpha)$, where η_α is the generalized friction coefficient [26]. The exact solution involves a double series with generalized regularized hypergeometric functions [24], from which two scaling forms can be distinguished in the limit of long measurement times,

$$\wp_a(t_a, t) \sim \begin{cases} t_a^{\alpha-1} t^{-\alpha}, & t_a \gg t \\ \left(x_0 T/[F K_\alpha] + t_a^\alpha/\Gamma(1+\alpha)\right) t^{-1-\alpha}, & t_a \ll t \end{cases} . \tag{8}$$

Similar to the result (5) for the first passage in a finite domain we obtain the crossover from the measurement time scaling with exponent $1+\alpha$ to α with increased aging, while the aging time appears explicitly for intermediate and strong aging. Fig. 3 shows excellent agreement of our exact result with simulations.

Quenched trap model. The quenched trap model [14] is often used as a physical model for CTRW processes with scale-free trapping times. In this lattice model each site is assigned a random energy value, taken from an exponential density $p(E) = T_g^{-1} \exp(-E/T_g)$, where we set the Boltzmann constant to unity. T_g is the system-specific 'glass' temperature setting the scale for the energy distribution $p(E)$ [14]. A sample realization for such a quenched energy landscape is displayed in Fig. 4. At lattice site x the walker faces the trap energy E_x and needs to escape by thermal fluctuations (Kramers escape). After escaping a trap, the walker jumps to one of the two nearest sites and is trapped again, see the schematic in Fig. 4. According to the Arrhenius law the trapping time at x becomes $\tau_x = \tau_0 \exp(E_x/T)$, where T is the bath temperature and τ_0 is an inverse microscopic rate of escape attempts. The combination of the density $p(E)$ with the Arrhenius law yields the long-tailed distribution of trapping times, $\psi(\tau) = \mu \tau_0^\mu \tau^{-1-\mu}$ with the scaling exponent $\mu = T/T_g$. When $T < T_g$, the quenched trap model thus leads to a power-law trapping time density with diverging characteristic trapping time $\langle\tau\rangle$ [14].

In the CTRW model individual trapping times τ all have the same distribution ψ but are independent variables, such that the system is renewed each time a new trapping time is drawn from ψ. This annealed form of the disorder contrasts the quenched nature of the trap model. A walker that leaves a trap may revisit it during later jumps, and the ensuing random walk thus exhibits correlations and is no renewal process. Such correlations are irrelevant in dimensions three and higher, as random walks are transient. To avoid such correlations in lower dimensions we equip the quenched landscape with the external bias force F [27]. This force tilts the quenched trap landscape (Fig. 4) and thus minimizes the likelihood that the walker returns to previously visited sites [14].

Our simulations included an initial aging routine, in which the walker moves along the lattice in a given realization of the quenched energy landscape with the additional bias due to the external force F. After the aging for the period t_a, an absorbing site is introduced, which is placed at a the distance x_0 from the walker, independent of its initial position on the lattice. The resulting first passage time is recorded, and this computer experiment

averaged over 10^5 realizations of the quenched landscape.

The result for the FPTD obtained from the simulations of the quenched trap model matches excellently with both the exact result and the simulation of the annealed CTRW model, as shown in Fig. 3. We thus expect that the first passage dynamics of an aged particle to a surface in unbiased quenched trap landscapes in three dimensions can be described by results (4) or (5) depending on whether the volume is finite or semi-infinite.

Conclusion. In this paper we studied the first passage dynamics of an aging diffusion process. In the CTRW model with scale-free trapping time distribution we showed how aging changes the scaling exponent of the measurement time t and how the aging time t_a appears in the FPTD. In the semi-infinite case we revealed three distinct scaling regimes, while on a finite domain and in the biased case two scaling regimes appear. Our exact results were demonstrated to agree perfectly with simulations of the CTRW process. In the biased case, the first passage dynamics measured in the quenched trap model showed excellent agreement with the CTRW approach.

A general feature observed in our results is that aging significantly reduces the efficiency of the first passage, as seen by the decrease of the slope of the FPTD in an aged system. This reflects a general property of processes with scale-free trapping times: as the system evolves, longer and longer trapping times appear on average and lead to a slowing-down of the dynamics. For free subdiffusion this corresponds to an effectively time-dependent diffusivity $K_{\rm eff} \simeq t^{\alpha-1}$. In the quenched trap model this would correspond to the particle finding an ever deeper trap during its motion across the energy landscape.

The first passage time represents one of the most fundamental concepts in stochastic processes. In many systems it is fairly easy to experimentally or numerically record the first passage dynamics. Our findings presented here for aged systems complement the classical results for the first passage dynamics in non-aged systems governed by scale-free trapping times. In condensed matter systems such as amorphous semiconductors aging is a relevant concern for applications, as it significantly changes the first passage dynamics and thus the signatures of the electrical current. As the age of amorphous semiconductors can be reliably controlled in experiment [16], such systems would be ideal to further test the CTRW model for charge carrier transport. In groundwater systems governed by scale-free trapping time distributions, the reduced first passage efficiency would imply an increased retention of potentially detrimental chemicals dissolved in the water. And, finally, in biological systems, aging effects and the associated population splitting lead to the progressive immobilization of particles with potentially relevant biological function [5, 10, 21, 31].

The lack of a characteristic trapping time of both the annealed aging CTRW process or the motion in the quenched energy landscape naturally makes the process non-stationary, a property, that in turn is closely related to the non-ergodicity of the system [32]. Using relatively simple experimental methods to probe the first passage statistics of a system, such as the charge carrier transport in amorphous semiconductors, as function of measurement and aging times would represent a direct way to determine the non-stationarity of a system.

With the rapid advance of single molecule tracking techniques it has become possible to diagnose experimentally recorded time series from individual particle trajectories with respect to the very stochastic mechanism behind the measured anomalous diffusion by various complementary tools [28–30, 33–35]. This information of the nature of some particle's dynamics, in particular, whether it is an ergodic or non-ergodic motion, then allows one to deduce important consequences for the systems such as the (ir)reproducibility of experiments or the dynamics of followup processes like the diffusion-limitation of reactions. With the characteristic crossovers between different scaling regimes of the measurement time t and the explicit aging time dependence the current results provide a powerful additional tool to probe the underlying stochastic mechanism. Moreover, given a sufficiently wide measurement window our results allow to read out the actual age t_a of the system from measured first passage data. This would be an extremely useful information for systems with unknown age.

AG acknowledges funding through an Alexander von Humboldt Fellowship. RM acknowledges funding from the Academy of Finland (FiDiPro scheme).

* Electronic address: rmetzler@uni-potsdam.de

[1] H. Scher and E. W. Montroll, Phys. Rev. B **15**, 2455 (1975).
[2] R. Steyrleuthner et al, Advanced Materials **22**, 2799 (2010).
[3] J.-P. Bouchaud and A. Georges, Phys. Rep. **195**, 12 (1990); R. Metzler and J. Klafter, *ibid.* **339**, 1 (2000); J. Phys. A **37**, R161 (2004).
[4] B. Berkowitz, A. Cortis, M. Dentz, and H. Scher, Rev. Geophys. **44**, RG2003 (2006); H. Scher, G. Margolin, R. Metzler, J. Klafter, and B. Berkowitz, Geophys. Res. Lett. **29**, 1061 (2002).
[5] S. M. A. Tabei et al, Proc. Natl. Acad. Sci. USA **110**, 4911 (2013); A. V. Weigel, B. Simon, M. M. Tamkun, and D. Krapf, Proc. Nat. Acad. Sci. USA **108**, 6438 (2011).
[6] J.-H. Jeon et al, Phys. Rev. Lett. **106**, 048103 (2011).
[7] I. Y. Wong et al., Phys. Rev. Lett. **92**, 178101 (2004); Q. Xu, L. Feng, R. Sha, N. C. Seeman, and P. M. Chaikin, Phys. Rev. Lett. **106**, 228102 (2011).
[8] X. Brokmann et al, Phys. Rev. Lett. **90**, 120601 (2003); G. Margolin and E. Barkai, J. Chem. Phys. **121**, 1566 (2004).
[9] J.-P. Bouchaud, J. Phys. I (Paris) **2**, 1705 (1992); G. Bel and E. Barkai, Phys. Rev. Lett. 94, 240602 (2005); A. Rebenshtok and E. Barkai, *ibid.* **99**, 210601 (2007); I. M.

Zaid, and R. Metzler, *ibid.* **98**, 200603 (2007).
[10] E. Barkai, Y. Garini, and R. Metzler, Physics Today **65**(8), 29 (2012).
[11] C. Monthus and J.-P. Bouchaud, J. Phys. A **29**, 3847 (1996); B. Rinn, P. Maass, and J.-P. Bouchaud, Phys. Rev. Lett. **84**, 5403 (2000).
[12] E. Barkai, *ibid.* **90**, 104101 (2003); E. Barkai and Y.-C. Cheng, J. Chem. Phys. **118**, 167 (2003).
[13] Note that certain aging effects still persist in the range $1 < \alpha < 2$ when $\langle\tau\rangle$ is finite bus ψ has diverging fluctuations: P. Allegrini et al, Phys. Rev. E **66**, 015101 (2002); *ibid.* **68**, 056123 (2003).
[14] E. Bertin and J.-P. Bouchaud, Phys. Rev. E **67**, 026128 (2003); S. Burov and E. Barkai, Phys. Rev. Lett. **98**, 250601 (2007).
[15] E. Barkai, Phys. Rev. Lett. **90**, 104101 (2003); T. Geisel and S. Thomae, *ibid.* **52**, 1936 (1984); G. Radons, Adv. Solid State Phys. **38**, 439 (1999).
[16] M. Schubert et al., Phys. Rev. B **87**, 024203 (2013).
[17] B. D. Hughes, Random walks and random environments, vol 1: random walks (Oxford University Press, Oxford, UK, 1995).
[18] The Laplace transform of a function $f(t)$ is defined as

$$f(u) = \mathscr{L}\{f(t); t \to u\} = \int_0^\infty f(t) \exp(-ut) dt.$$

[19] R. Metzler and J. Klafter, Physica A **278**, 107 (2000)
[20] S. Redner, A guide to first-passage processes (Cambridge University Press, Cambridge, UK 2001).
[21] J. Schulz, E. Barkai, and R. Metzler, Phys. Rev. Lett. **110**, 020602 (2013); Phys. Rev. X, at press.
[22] This transform is defined in terms of

$$P_a(k,s,u) = \mathscr{L}\left\{\mathscr{L}\left\{\int_{-\infty}^{\infty} P_a(x,t_a,t) e^{ikx} dx; t_a \to s\right\}; t \to u\right\}.$$

[23] J. Klafter and I. M. Sokolov, First steps in random walks: from tools to applications (Cambridge University Press, Cambridge, UK, 2011).
[24] H. Krüsemann, A. Godec, and R. Metzler (unpublished).
[25] Note that we use the symbol $l_{k\alpha}(z)$ here for a function, that is formally defined in terms of its Laplace image as $l_{k\alpha}(u) = \exp(-u^{k\alpha})$. When $k\alpha > 1$, this is no longer a one-sided stable law.
[26] R. Metzler, E. Barkai, and J. Klafter, Phys. Rev. Lett. **82**, 3563 (1999).
[27] S. Burov and E. Barkai, Phys. Rev. E **86**, 041137 (2012).
[28] M. Magdziarz, A. Weron, K. Burnecki, and J. Klafter, Phys. Rev. Lett. **103**, 180602 (2009); K. Burnecki et al, Biophys. J. **103**, 1839 (2012).
[29] S. Condamin, V. Tejedor, R. Voituriez, O. Bénichou, and J. Klafter, Proc. Natl. Acad. Sci. USA **105**, 5675 (2008).
[30] I. M. Sokolov, Soft Matter **8**, 9043 (2012); F. Thiel, F. Flegel, and I. M. Sokolov, Phys. Rev. Lett. **111**, 010601 (2011).
[31] A. V. Weigel, M. M. Tamkun, and D. Krapf, Proc. Natl. Acad. Sci. USA **110**, E4591 (2013).
[32] S. Burov and E. Barkai, Phys. Rev. Lett. **98**, 250601 (2007); S. Burov, R. Metzler, and E. Barkai, Proc. Natl. Acad. Sci USA **107**, 13228 (2010).
[33] V. Tejedor et al, Biophys. J. **98**, 1364 (2010); Y. He, S. Burov, R. Metzler, and E. Barkai, Phys. Rev. Lett. **101**, 058101 (2008); S. Burov, J.-H. Jeon, R. Metzler, and E. Barkai, Phys. Chem. Chem. Phys. **13**, 1800 (2011); J.-H. Jeon, E. Barkai, and R. Metzler, J. Chem. Phys. **139**, 121916 (2013); A. Cherstvy, A. V. Chechkin, and R. Metzler, Soft Matter, DOI: 10.1039/C3SM52846D.
[34] T. Albers and G. Radons, EPL **102**, 40006 (2013); M. Heidernaetsch, M. Bauer, and G. Radons, J. Chem. Phys. **139**, 184105 (2013).
[35] A. M. Berezhkovskii, L. Dagdug, and S. M. Bezrukov, Biophys. J. **106**, L09 (2014); M. Saxton, *ibid.* **103**, 2411 (2012); Biophys. J. **72**, 1744 (1997).